Journal of Computational and Applied Mathematics 234 (2010) 593–604

Contents lists available at ScienceDirect

Journal of Computational and Applied Mathematics

journal homepage: www.elsevier.com/locate/cam

Assessment of subgrid-scale models for the incompressible Navier–Stokes equations☆

Yan Zhang, Yinnian He*

Faculty of Science, State Key Laboratory of Multiphase Flow, Xi'an Jiaotong University, Shaanxi, 710049, PR China

ARTICLE INFO

Article history:
Received 10 September 2009
Received in revised form 21 December 2009

Keywords:
Navier–Stokes equations
Subgrid model
Eddy viscosity
Pressure stabilization method
Error analysis
Numerical tests

ABSTRACT

In this paper, we assess two kinds of subgrid finite element methods for the two-dimensional (2D) incompressible Naver-Stokes equations (NSEs). These methods introduce subgrid-scale (SGS) eddy viscosity terms which do not act on the large flow structures. The eddy viscous terms consist of the fluid flow fluctuation strain rate stress tensors. The fluctuation tensor can be calculated by a elliptic projection or a simple L^2 projection (projective filter) in finite element spaces. The finite element pair P_2/P_1 is adopted to numerically implement analysis and computation. We give a complete error analysis based on the assumptions of some regularity conditions. On the part of numerical tests, the numerical computations for the stationary flows show that the numerical results agree with some benchmark solutions and theoretical analysis very well. Furthermore, the given SGS models are applied to the non-stationary fluid flows.

1. Introduction

In this paper, we focus on formulating two kinds of subgrid eddy viscosity models for the incompressible Navier–Stokes equations. For subgrid models, it is admitted that there exists a scale separation between large and small scales. These models can be viewed as a viscous correction for large scale fluid flows. For the laminal fluid flows, the added SGS viscous terms should not affect the large scale structures of fluid flow fields and should tend to vanish. These SGS models are flexible and effective for high Reynolds number fluid flows and can suppress the spurious fluctuations of flow fields.

It is well-known that, for most problems of fluid flows, the numerical algorithms capturing all scales of fluid flows are impossible and there exist several scales that span from the large scales to the small Kolmogorov scales which can hardly be resolved by state-of-the-art computers for most engineering problems very efficiently. For most low viscosity flows (high Reynolds number flows), the nonlinear transport term dominates the fluid flows and the coercivity constant of the second-order dissipative term in NSEs goes to zero. Then, the spurious oscillations will spread throughout the entire computational domain. It will become very difficult for the generally used pure Galerkin methods to solve these problems. In the numerical simulations of scientific and engineering applications, the eddy viscosity models are often utilized to solve the convection-dominated NSE by researchers and engineers, which have been achieved many successes in engineering practice [1]. These kinds of models are firstly proposed in [2], developed in [3], and introduced a dissipative mechanism in [4]. At present, these models have been further improved by various numerical methods [5–7]. In their models, the scale separation is based on L^2 and elliptic projection from two-level finite element spaces. For the convection term, the stabilization term is mainly from subscale velocity deformation tensor. Recently, Hughes et al. have proposed a variational multi-scale method (VMM)

☆ This work is supported by Chinese NSF (Grant No. 10971166) and the National Basic Research Program of China (Grant No. #2005CB321703).
* Corresponding author.
E-mail addresses: yanzhxj@gmail.com (Y. Zhang), heyn@mail.xjtu.edu.cn (Y. He).

0377-0427/$ – see front matter © 2010 Elsevier B.V. All rights reserved.
doi:10.1016/j.cam.2009.12.051

in which the diffusion acts only on the finest resolved scales. There are different ways of how to define coarse and small scales according to VMM framework [8]. It must be mentioned that the referred SGS methods can be regarded as VMM.

In this paper, we will give two SGS models to stabilize the flow fields and suppress the spurious oscillations from resolved small scales by virtue of an elliptic projection and a L^2 projection. The SGS terms are easily implemented, and do not need complex computational methods. Meanwhile, these models are easily extended to engineering applications.

The P_2/P_1 finite element pair is adopted to approach velocity–pressure fields. Then we show its well-posedness and derive optimal error estimates. For low Reynolds number fluid flows, the results indicate that this method has a convergence rate of the same order as the standard Garlerkin method. For high Reynolds number (Re) fluid flows, we give some comparisons with the classical benchmark solutions. By the numerical tests, it is shown that the proposed subgrid correction models can simulate the high Reynolds fluid flows very effectively and can numerically correct computational results.

The outline of this paper is organized as follows. In Section 2, we give the NSEs and the corresponding functional settings. In Section 3, the SGS viscous terms are introduced into NSEs and the standard Galerkin discretization of the Navier–Stokes problem are given. In Section 4, we show the results of the error estimates. Some numerical results are presented in Section 5, which show the correctness and efficiency of the methods. Finally, we give some conclusions.

2. Navier–Stokes equations and functional settings

Let $\Omega \subset \mathbb{R}^2$ be a polygonal domain with Lipschitz continuous boundary $\Gamma = \partial\Omega$. We consider the stationary Navier–Stokes equations

$$\begin{cases} -\nu\Delta u + \nabla p + (u\cdot\nabla)u = f, & \text{in } \Omega \\ \operatorname{div} u = 0, & \text{in } \Omega \\ u = 0, & \text{on } \Gamma \end{cases} \tag{1}$$

where $u = (u_1, u_2)$ represents the velocity vector, p is the pressure, f is the body force and $\nu > 0$ stands for the viscosity.

We introduce the following functional settings

$$X := H_0^1(\Omega)^2, \qquad V := \{v \in X, \operatorname{div} v = 0\}, \qquad Y = (L^2(\Omega))^2,$$
$$Q := L_0^2(\Omega) = \left\{ q \in L^2(\Omega) : \int_\Omega q\mathrm{d}x = 0 \right\}.$$

We denote by $(\cdot,\cdot)$ and $\|\cdot\|_0$ the inner product and norm in $L^2(\Omega)$ or $L^2(\Omega)^2$. The space $H^k(\Omega)$ or $H^k(\Omega)^2$ denotes the standard Sobolev spaces with norm $\|\cdot\|_k$ and semi-norm $|\cdot|_k$. The space $H_0^1(\Omega)$ or $H_0^1(\Omega)^2$ is equipped with the following product and norm

$$((u, v)) = (\nabla u, \nabla v), \qquad |u|_1 = ((u, u))^{1/2}.$$

The space $H^{-1}(\Omega)$ is the dual space of $H_0^1(\Omega)$ equipped with the norm

$$\|z\|_{-1} = \sup_{v\in H_0^1(\Omega)} \frac{|(z, v)|}{\|\nabla v\|_0}.$$

For convenience, we introduce the following bilinear form $a(\cdot,\cdot)$ on $X \times X$ which is coercive in X: There exists a constant $0 < C_0 \le 1$ such that

$$a(u, u) = ((u, u)) \ge C_0\|\nabla u\|_0^2, \quad \forall\, u \in X, \tag{2}$$

and $d(\cdot,\cdot)$ on $X \times Q$ defined by

$$d(v, q) = (q, \operatorname{div} v), \quad \forall\, v \in X,\ q \in Q.$$

The trilinear term is defined by

$$\begin{aligned} b(u; v, w) &= ((u\cdot\nabla)v, w) + \frac{1}{2}((\operatorname{div} u)v, w) \\ &= \frac{1}{2}((u\cdot\nabla)v, w) - \frac{1}{2}((u\cdot\nabla)w, v), \quad \forall\, u, v,\ w \in X, \end{aligned}$$

which is the skew-symmetric form of the convective term. It is easy to gain

$$b(u; v, w) = -b(u; w, v). \tag{3}$$

Also, we have the following estimates [9]

$$|b(u; v, w)| \le N\|\nabla u\|_0\|\nabla v\|_0\|\nabla w\|_0, \quad \forall\, u, v,\ w \in X, \tag{4}$$

where N is a positive constant depending only on the domain Ω. For a given $f \in (H^{-1}(\Omega))^2$, the weak form of Eq. (1) reads as:

Find $(u, p) \in (X, Q)$ such that

$$\begin{aligned} &\nu a(u, v) + b(u; u, v) - d(v, p) = (f, v), \quad \forall\, v \in X, \\ &d(u, q) = 0, \qquad\qquad\qquad\qquad\quad \forall\, q \in Q. \end{aligned} \tag{5}$$

The Lax–Milgram theorem and the inf–sup condition [10]

$$\sup_{v \in X} \frac{\mathrm{d}(v, q)}{\|\nabla v\|_0} \geq \beta_1 \|q\|_0, \tag{6}$$

where β_1 is positive constant, guarantee that there is a unique solution of (5).

For the finite element analysis, we need some existence, uniqueness and regularity properties of the solution for the Navier–Stokes equations.

Theorem 2.1. *Given a function $f \in (H^{-1}(\Omega))^2$, there exists at least one solution (u, p) satisfying the Navier–Stokes problem (5) and*

$$u \in X, \qquad p \in Q, \tag{7}$$

(see [10,11]). In addition, if f and ν satisfy the following uniqueness condition:

$$N\|f\|_{-1} \leq C_0 \nu^2, \tag{8}$$

then the Navier–Stokes problem (5) has a unique solution $(u, p) \in X \times Q$ (see [10,11]).

Finally, if $f \in H^1(\Omega)^2$ and (8) hold, then the solution (u, p) satisfies that

$$\nu\|u\|_3 + \|p\|_2 \leq c\|f\|_1, \tag{9}$$

(see [9]), where c is a general positive constant depending on the domain Ω, which stands for different values at different occurrences.

If we restrict the domain Ω to be a convex, polygonal domain in a 2-dimensional plane, Theorem 2.1 is invalid. So, for the current polygonal domain, we make the following regularity assumption of the solution (u, p) of Eq. (1):

Assumption 2.1. When the domain Ω is a convex, polygonal domain in a 2-dimensional plane, we assume that (u, p) satisfies

$$u \in X \cap H^3(\Omega)^2, \qquad p \in Q \cap H^2(\Omega). \tag{10}$$

If $f \in H^1(\Omega)^2$ and (8) hold, then the solution (u, p) satisfies that

$$\nu\|u\|_3 + \|p\|_2 \leq c\|f\|_1, \tag{11}$$

where c is a positive constant depending on the domain Ω, which stands for different values at different occurrences.

If we implement the finite element discretization for the Navier–Stokes equation (1), the computational domain will become a polygonal domain. Under this case, we will use regularity results of Assumption 2.1 to carry out the related analysis in the rest sections.

3. Discretization of Navier–Stokes equations and Subgrid model

We give a family τ_h, which is a triangle or quadrilateral partition of Ω, assumed to be regular in the usual sense [11]. The diameter of the cell K is denoted by h_K. The mesh parameter h describes the maximum diameter of the cells $K \in \tau_h$.

We introduce the finite-dimensional subspace X_h and Q_h,

$$\begin{aligned} &X_h := \{v_h \in (C^0(\Omega))^2 \cap X : v_h|_K \in P_2(K)^2, \forall\, K \in \tau_h\}, \\ &Q_h := \{q_h \in Q : q_h|_K \in P_1(K), \forall\, K \in \tau_h\}, \end{aligned} \tag{12}$$

where $P_l(K)$ denotes the set of polynomials of $\mathbb{R}^2$ of degree $\leq l$ on the cell K. We define the discrete analogue of the space V denoted by V_h

$$V_h := \{v_h \in X_h : d(v_h, q_h) = 0, \forall\, q_h \in Q_h\}. \tag{13}$$

Then we assume that, for the finite element space (X_h, Q_h), the following approximation properties hold: For $(u, p) \in (H^3(\Omega)^2 \cap X, H^2(\Omega) \cap Q)$,

$$\begin{aligned} &\inf_{v_h \in X_h} \{\|u - v_h\|_0 + h\|\nabla(u - v_h)\|_0\} \leq ch^3|u|_3, \\ &\inf_{q_h \in Q_h} \|p - q_h\|_0 \leq ch^2|p|_2. \end{aligned} \tag{14}$$

Meanwhile, the velocity–pressure pair in (X_h, Q_h) satisfies the following discrete inf–sup condition [12]

$$\inf_{q_h \in Q_h} \sup_{v_h \in X_h} \frac{\mathrm{d}(v_h, q_h)}{\|q_h\|_0 \|\nabla v_h\|_0} \geq \beta > 0. \tag{15}$$

Remark 3.1 ([12]). We define a projection operator for all elements in X. For all $u \in X$, we define $P_{1,h}u \in R_1$ so that

$$((P_{1,h}u, v)) = ((u, v)), \quad \forall\, v \in R_1, \tag{16}$$

which has the following properties

$$\|P_{1,h}v\|_1 \le c\|v\|_1, \quad \forall\, v \in X, \tag{17}$$

$$\|\nabla(I - P_{1,h})v\|_0 < c\|\nabla v\|_0, \quad \forall\, v \in X, \tag{18}$$

$$\|v - P_{1,h}v\|_1 \le ch\|v\|_2, \quad \forall\, v \in H^2(\Omega)^2 \cap X, \tag{19}$$

$$\|v - P_{1,h}v\|_1 \le ch^l\|v\|_{1+l}, \quad 1 \le l \le k,\ \forall\, v \in H^2(\Omega)^2 \cap X, \tag{20}$$

where $R_1 = \{v \in (C^0(\Omega))^2 \cap X : v_h|_K \in P_1(K)^2, \forall\, K \in \tau_h\}$. The projection operator $P_{1,h}$ is called as the elliptic projection operator.

We know that, for high Reynolds number fluid flows, when the fluid convection dominates fluid flow fields, under the non-adequate resolution of meshes, the flow field will become very unstable. When the mesh scales cannot resolve the smallest scale in fluid flows, we must add some term into Navier–Stokes equations to smear out the effect from the unresolved scales. Here, we chose the following subgrid stabilization term to control the effect from the unresolved scales

$$M(u, v) = \alpha(\nabla(I - P_{1,h})u, \nabla(I - P_{1,h})v), \quad \forall\, u, v \in X, \tag{21}$$

where α is the user-selected stabilization parameter and typically, $\alpha = h^s$ (s is a real number). This subgrid stabilization term is based on the elliptic projection. An analogous SGS model is used to solve the convection-dominated convection diffusion problems in [13]. But, the proposed SGS model in this paper is different from the SGS model in [13]. The SGS model in [13] is based on two-grid finite element spaces and our model is constructed from.

The above SGS term $M(\cdot, \cdot)$ is defined according to the elliptic projection. Now, we give another definition based on the L^2 projection. Let $Q_{1,h} : X \to R_1$ be a L^2 projection. For all $u \in X$, $Q_{1,h}$ is defined such that for all $v \in R_1$,

$$(Q_{1,h}u, v) = (u, v). \tag{22}$$

So, we can define another simple SGS term as follows

$$M_l(u, v) = \alpha_l(\nabla(I - Q_{1,h})u, \nabla(I - Q_{1,h})v), \quad \forall\, u, v \in X, \tag{23}$$

where $\alpha_l = h^s$ (s is a real number).

Lemma 3.1 ([13]). *$P_{1,h}$ and $Q_{1,h}$ are the orthogonal projections with respect to the H^1 and L^2 inner product. The, for any $w \in X$*

$$\nabla P_{1.h}w = Q_{1,h}\nabla w. \tag{24}$$

Using the stabilization term Eq. (21), we give the following stabilization finite element discretization form of the variational form (5): find $(u_h, q_h) \in (X_h, Q_h)$ satisfying

$$\begin{aligned} &\nu a(u_h, v_h) + b(u_h; u_h, v_h) - d(v_h, p_h) + M(u_h, v_h) = (f, v_h), && \forall\, v_h \in X_h, \\ &d(u_h, q_h) = 0, && \forall\, q_h \in Q_h. \end{aligned} \tag{25}$$

Under the inf–sup condition (15), the formulation (25) is equivalent to the following problem [11]: find $u_h \in V_h$ such that

$$\nu a(u_h, v_h) + b(u_h; u_h, v_h) + M(u_h, v_h) = (f, v_h), \quad \forall\, v_h \in V_h. \tag{26}$$

Theorem 3.1 ([11]). *Suppose the uniqueness condition (8) holds. Under the condition (15), then the variational form (25) has a unique solution $(u_h, p_h) \in (X_h, Q_h)$.*

4. Error analysis

The basic principle of subgrid method focuses on enhancing the numerical stability of solving discrete Navier–Stokes equations. For this purpose, we will analyze the numerical scheme (25) by H^1 and L^2 estimates of velocity and L^2 estimate of pressure. The following given analysis is classical [9,13,14]. To derive error estimates of the finite element solution (u_h, p_h), we first give the following lemma.

Lemma 4.1. *The finite element approximation of velocity for (25) is stable*

$$\nu\|\nabla u_h\|_0^2 + 2\alpha\|\nabla(I - P_{1,h})u_h\|_0^2 \le \frac{1}{\nu\sqrt{C_0}}\|f\|_{-1}^2, \tag{27}$$

where C_0 is the constant of (2).

Proof. The result is easily obtained by setting $v_h = u_h$, $p_h = q_h$ in (25) and Cauchy Schwarz, Young's inequalities. □

Theorem 4.1. *Assuming the uniqueness condition (8) holds, then we have*

$$\nu\|\nabla(u-u_h)\|_0^2 + 2\alpha\|\nabla(I-P_{1,h})(u-u_h)\|_0^2 \le C \inf_{w_h\in V_h}\left\{\nu\|\nabla(u-w_h)\|_0^2 + \frac{N^2}{\nu}(\|\nabla u\|_0 + \|\nabla u_h\|_0)^2\|\nabla(u-w_h)\|_0^2 \right.$$
$$\left. + \alpha\|\nabla(I-P_{1,h})u\|_0^2 + \alpha\|\nabla(I-P_{1,h})(u-w_h)\|_0^2\right\} + C\inf_{q_h\in Q_h}\frac{1}{\nu}\|p-q_h\|_0^2, \tag{28}$$

where C is independent of ν, α *and h.*

Proof. First, we know that the true solution satisfies the following equation

$$\nu a(u, v_h) + b(u; u, v_h) - d(v_h, p) - d(u, q_h) + M(u, v_h) = (f, v_h) + M(u, v_h), \quad \forall\, v_h \in X_h,\ q_h \in Q_h. \tag{29}$$

By subtracting Eq. (25) from Eq. (29):

$$\nu a(u-u_h, v_h) + b(u; u, v_h) - b(u_h; u_h, v_h) - d(v_h, p-p_h) - d(u-u_h, q_h) + M(u-u_h, v_h) = M(u, v_h),$$
$$\forall\, v_h \in X_h,\ q_h \in Q_h. \tag{30}$$

Now, let $u - u_h = \eta - \phi_h$, with $\eta = u - w_h$ and $\phi_h = u_h - w_h$, where w_h is the any function in V_h. Taking $v_h = \phi_h \in V_h$ in Eq. (30), we obtain:

$$\begin{aligned}\nu a(\phi_h, \phi_h) + M(\phi_h, \phi_h) =\ & \nu a(\eta, \phi_h) + b(u; u, \phi_h) - b(u_h; u_h, \phi_h)\\ & + M(\eta, \phi_h) - d(\phi_h, p-q_h) - M(u, \phi_h), \quad \forall\, q_h \in Q_h.\end{aligned} \tag{31}$$

To bound the nonlinear terms, we rewrite these terms as follows:

$$b(u; u, \phi_h) - b(u_h; u_h, \phi_h) = b(u; \eta, \phi_h) + b(\eta; u_h, \phi_h) - b(\phi_h; u_h, \phi_h). \tag{32}$$

By using Eq. (4), Young's inequality, Eqs. (27) and (8), we have:

$$\begin{aligned}|b(u; u, \phi_h) - b(u_h; u_h, \phi_h)| &\le N(\|\nabla u\|_0 + \|\nabla u_h\|_0)\|\nabla\eta\|_0\|\nabla\phi_h\|_0 + N\|\nabla u_h\|_0\|\nabla\phi_h\|_0^2\\ &\le \frac{CN^2}{\nu}(\|\nabla u\|_0 + \|\nabla u_h\|_0)^2\|\nabla\eta\|_0^2 + \frac{1}{4}\nu\|\nabla\phi_h\|_0^2.\end{aligned} \tag{33}$$

To bound the linear terms in the right-hand side of Eq. (31), by the Cauchy Schwarz inequality and Young's inequality, we get

$$|\nu a(\eta, \phi_h)| \le \nu\|\nabla\eta\|_0\|\nabla\phi\|_0 \le \nu\|\nabla\eta\|_0^2 + \frac{1}{4}\nu\|\nabla\phi_h\|_0^2, \tag{34}$$

$$|d(\phi_h, p-q_h)| \le \nu\|p-q_h\|_0^2 + \frac{1}{4}\nu\|\nabla\phi_h\|_0^2, \tag{35}$$

$$\begin{aligned}|M(\eta, \phi_h)| &\le \alpha\|\nabla(I-P_{1,h})\eta\|_0\|\nabla(I-P_{1,h})\phi_h\|_0\\ &\le \frac{\alpha}{4}\|\nabla(I-P_{1,h})\phi_h\|_0^2 + \alpha\|\nabla(I-P_{1,h})\eta\|_0^2,\end{aligned} \tag{36}$$

and

$$|M(u, \phi_h)| \le \alpha\|\nabla(I-P_{1,h})u\|_0^2 + \frac{\alpha}{4}\|\nabla(I-P_{1,h})\phi_h\|_0^2. \tag{37}$$

Combining Eqs. (33)–(37) with Eq. (31) gives

$$\nu\|\nabla\phi_h\|_0^2 + 2\alpha\|\nabla(I-P_{1,h})\phi_h\|_0^2 \le C\left\{\nu\|\nabla\eta\|_0^2 + \frac{N^2}{\nu}(\|\nabla u\|_0 + \|\nabla u_h\|_0)^2\|\nabla\eta\|_0^2 + \alpha\|\nabla(I-P_{1,h})\eta\|_0^2\right.$$
$$\left. + \alpha\|\nabla(I-P_{1,h})u\|_0^2 + \frac{1}{\nu}\|p-q_h\|_0^2\right\}. \tag{38}$$

The final result is easily obtained by using the triangle inequality

$$\begin{aligned}\nu\|\nabla(u-u_h)\|_0^2 + 2\alpha\|\nabla(I-P_{1,h})(u-u_h)\|_0^2 \le\ & C\{\nu\|\nabla(u-w_h)\|_0^2 + 2\alpha\|\nabla(I-P_{1,h})(u-w_h)\|_0^2\\ & + \nu\|\nabla\phi_h\|_0^2 + 2\alpha\|\nabla(I-P_{1,h})\phi_h\|_0^2\}.\end{aligned} \tag{39}$$

□

By choosing the proper parameters α and h, and using Eq. (14) and Remark 3.1, we can obtain the following corollary:

Corollary 4.1. *Under the assumption of Theorem 3.1, Remark 3.1 and the regularity assumption of* $(u, p) \in (H^3(\Omega)^2 \cap X, H^2(\Omega) \cap Q)$ *in Theorem 2.1, there exists a constant C independent of* α *and h such that:*

$$\nu\|\nabla(u-u_h)\|_0^2 + 2\alpha\|\nabla(I-P_{1,h})(u-u_h)\|_0^2 \le Ch^4|u|_3^2\left(\nu + \frac{1}{\nu}\left(1+\frac{1}{\nu}\right)^2 + \alpha\right) + \frac{C}{\nu}h^4|p|_2^2 + C\alpha h^2|u|_3^2. \tag{40}$$

In particular,

$$\|\nabla(u-u_h)\|_0 \le Ch^2, \quad \text{if } \alpha = h^2. \tag{41}$$

Now, we give the estimation of the discrete pressure in the following theorem:

Theorem 4.2. *Supposing the uniqueness condition (8) holds, then the error estimate of pressure field satisfies*

$$\begin{aligned}\|p-p_h\|_0 \le\ & C((\nu+1)\|\nabla(u-u_h)\|_0 + \|\nabla(u-u_h)\|_0^2 + \alpha\|\nabla(I-P_{1,h})(u-u_h)\|_0 \\ & + \alpha\|\nabla(I-P_{1,h})u\|_0) + C\inf_{q_h\in Q_h}\|p-q_h\|_0,\end{aligned} \tag{42}$$

where C is independent of ν, α *and h.*

Proof. Setting the error of the velocity $e = u - u_h$ and introducing an approximation of the pressure $\widetilde{p_h} \in Q_h$ in Eq. (30), we have:

$$d(v_h, p_h - \widetilde{p_h}) = d(v_h, p - \widetilde{p_h}) - \nu a(e, v_h) - (b(u; u, v_h) - b(u_h; u_h, v_h)) - M(e, v_h) + M(u, v_h), \quad \forall\, v_h \in X_h. \tag{43}$$

From Eq. (4), the nonlinear terms are bounded as:

$$\begin{aligned}|b(u; u, v_h) - b(u_h; u_h, v_h)| &= |b(u; e, v_h) + b(e; u, v_h) - b(e; e, v_h)| \\ &\le C(\|\nabla e\|_0 + \|\nabla u\|_0)\|\nabla e\|_0\|\nabla v_h\|_0.\end{aligned} \tag{44}$$

To bound the linear terms in the right-hand side of Eq. (43), we apply Cauchy Schwarz inequality and Remark 3.1, the term $M(u, v_h)$ is bounded as in the inequality (36). From Eq. (44), we have

$$\begin{aligned}|d(v_h, p_h - \widetilde{p_h})| \le\ & C\{\|p-\widetilde{p_h}\|_0 + \nu\|\nabla e\|_0 + (\|\nabla e\|_0 + \|\nabla u\|_0)\|\nabla e\|_0 \\ & + \alpha\|\nabla(I-P_{1,h})e\|_0 + \alpha\|\nabla(I-P_{1,h})u\|_0\}\|\nabla v_h\|_0.\end{aligned} \tag{45}$$

Meanwhile, the inf–sup condition (15) implies that there exists a velocity $v_h \in X_h$ such that

$$d(v_h, p_h - \widetilde{p_h}) \ge \beta\|\nabla v_h\|_0\|p_h - \widetilde{p_h}\|_0. \tag{46}$$

In view of (46), we get

$$\|p-p_h\|_0 \le \|p-\widetilde{p_h}\|_0 + \beta^{-1}\frac{|d(v_h, p_h-\widetilde{p_h})|}{\|\nabla v_h\|_0}. \tag{47}$$

By Eqs. (45) and (47), we obtain the conclusion

$$\|p-p_h\|_0 \le C\|p-\widetilde{p_h}\|_0 + C(\nu\|\nabla e\|_0 + \|\nabla e\|_0^2 + \|\nabla e\|_0\|\nabla u\|_0 + \alpha\|\nabla(I-P_{1,h})e\|_0 + \alpha\|\nabla(I-P_{1,h})u\|_0). \tag{48}$$

Namely

$$\begin{aligned}\|p-p_h\|_0 \le\ & C((\nu+1)\|\nabla(u-u_h)\|_0 + \alpha\|\nabla(I-P_{1,h})(u-u_h)\|_0 + \alpha\|\nabla(I-P_{1,h})u\|_0 \\ & + \|\nabla(u-u_h)\|_0^2) + C\inf_{q_h\in Q_h}\|p-q_h\|_0. \quad \square\end{aligned} \tag{49}$$

Corollary 4.2. *Form Theorem 4.1, the approximation result (14), and Corollary 4.1, we have*

$$\|p-p_h\|_0 \le C(h^2 + \alpha^{\frac{1}{2}}h). \tag{50}$$

In particular,

$$\|p-p_h\|_0 \le Ch^2, \quad \text{if } \alpha = h^2, \tag{51}$$

where C is independent of α, *h.*

In order to derive the L^2 estimate for the velocity, we consider the linearized dual problem of the Navier–Stoles Eq. (1): given $\xi \in L^2(\Omega)$, find (ϕ, φ) such that

$$\nu a(\phi, v) + b(u; v, \phi) + b(v; u, \phi) + M(\phi, v) - d(v, \varphi) + d(\phi, q) = (\xi, v), \quad \forall\, (v, q) \in (X, Q). \tag{52}$$

Assuming that, for any $\xi \in L^2(\Omega)^2$, there exists a unique pair $(\phi, \varphi) \in (H^2(\Omega)^2 \cap X, H^1(\Omega) \cap Q)$ satisfying

$$\|\phi\|_2 + \|\varphi\|_1 \le C\|\xi\|_0. \tag{53}$$

Now we give the L^2 error estimate in the following theorem.

Theorem 4.3. *Supposing that the assumption of Theorems 4.1 and 4.2 hold, the dual problem (52) satisfies Eq. (53). We have*

$$\|u - u_h\|_0 \le Ch(1+\alpha)\|\nabla e\|_0 + C\|\nabla e\|_0^2 + C\alpha h^2 + Ch\|p - p_h\|_0, \tag{54}$$

where C is independent of α and h.

Proof. Setting $e = u - u_h$, and subtracting Eq. (29) from Eq. (25), we can get:

$$\begin{aligned} &\nu a(e, v_h) + b(u; u, v_h) - b(u_h; u_h, v_h) - d(v_h, p - p_h) \\ &\quad - d(e, q_h) + M(e, v_h) - M(u, v_h) = 0, \quad \forall\, v_h \in X_h,\ \forall\, q_h \in Q_h. \end{aligned} \tag{55}$$

Taking $\xi = e, v = e, q = p_h - p$ in Eq. (52) and subtracting Eq. (55), then we gain:

$$\begin{aligned} \|e\|_0^2 &\le |\nu a(\phi - v_h, e)| + |b(e; u, \phi) + b(u; e, \phi) - b(u; u, v_h) + b(u_h; u_h, v_h)| + |d(e, \varphi - q_h)| \\ &\quad + |d(\phi - v_h, p - p_h)| + |M(\phi - v_h, e) + M(u, v_h)| \\ &\le C(\nu\|\nabla e\|_0 + \|p - p_h\|_0 + \alpha\|\nabla(I - P_{1,h})e\|_0)\|\nabla(\phi - v_h)\|_0 + C\|\varphi - q_h\|_0\|\nabla e\|_0 \\ &\quad + \alpha\|\nabla(I - P_{1,h})u\|_0\|\nabla(I - P_{1,h})v_h\|_0 + |b(e; u, \phi) + b(u; e, \phi) - b(u; u, v_h) + b(u_h; u_h, v_h)|. \end{aligned} \tag{56}$$

Let $(\widetilde{\phi}, \widetilde{\varphi}) \in (X_h, Q_h)$ be the best approximation of $(\phi, \varphi) \in (H^2(\Omega)^2 \cap X, H^1(\Omega) \cap Q)$, we have the following approximation properties:

$$\begin{aligned} &\|\phi - \widetilde{\phi}\|_1 \le Ch\|\phi\|_2, \\ &\|\varphi - \widetilde{\varphi}\|_0 \le Ch\|\varphi\|_1. \end{aligned} \tag{57}$$

Setting $(v_h, q_h) = (\widetilde{\phi}, \widetilde{\varphi})$ and using the Cauchy–Schwarz inequality and the above approximation properties, Eq. (56) becomes:

$$\begin{aligned} \|e\|_0^2 &\le Ch(\|\nabla e\|_0 + \|p - p_h\|_0 + \alpha\|\nabla(I - P_{1,h})e\|_0)\|\phi\|_2 + Ch\|\varphi\|_1\|\nabla e\|_0 \\ &\quad + \alpha\|\nabla(I - P_{1,h})u\|_0\|\nabla(I - P_{1,h})\widetilde{\phi}\|_0 + |b(u; e, \phi) + b(e; u, \phi) - b(u; u, \widetilde{\phi}) + b(u_h; u_h, \widetilde{\phi})|. \end{aligned} \tag{58}$$

Using Remark 3.1 and (57), the consistent error term in the right-hand side of (58) gives

$$\begin{aligned} \alpha\|\nabla(I - P_{1,h})u\|_0\|\nabla(I - P_{1,h})\widetilde{\phi}\|_0 &= \alpha\|\nabla(I - P_{1,h})u\|_0\|\nabla(\widetilde{\phi} - \phi) + \nabla(\phi - P_{1,h}\widetilde{\phi})\|_0 \\ &\le \alpha\|\nabla(I - P_{1,h})u\|_0(\|\widetilde{\phi} - \phi\|_1 + \|\phi - P_{1,h}\phi\|_1 + \|P_{1,h}\phi - P_{1,h}\widetilde{\phi}\|_1) \\ &\le C\alpha h\|u\|_2(\|\widetilde{\phi} - \phi\|_1 + \|\phi - P_{1,h}\phi\|_1 + c\|\phi - \widetilde{\phi}\|_1) \\ &\le C\alpha h^2\|u\|_2\|\phi\|_2 \le C\alpha h^2\|u\|_3\|\phi\|_2. \end{aligned} \tag{59}$$

To bound the nonlinear terms in (58), we rewrite these terms as follows:

$$\begin{aligned} &b(u; e, \phi) + b(e; u, \phi) - b(u; u, \widetilde{\phi}) + b(u_h; u_h, \widetilde{\phi}) \\ &\quad = b(e; e, \phi) + b(u; e, \phi - \widetilde{\phi}) + b(e; u, \phi - \widetilde{\phi}) + b(e; e, \phi - \widetilde{\phi}). \end{aligned} \tag{60}$$

Using Eqs. (4) and (57), we gain

$$\begin{aligned} |b(u; e, \phi) + b(e; u, \phi) - b(u; u, \widetilde{\phi}) + b(u_h; u_h, \widetilde{\phi})| &\le C\|\nabla e\|_0^2\|\phi\|_1 + C\|\nabla u\|_0\|\nabla e\|_0\|\phi - \widetilde{\phi}\|_1 + C\|\nabla e\|_0^2\|\phi - \widetilde{\phi}\|_1 \\ &\le C(\|\nabla e\|_0 + h)\|\nabla e\|_0\|\phi\|_2. \end{aligned} \tag{61}$$

Combining all the bounds and Eq. (53) gives the final result

$$\begin{aligned} \|e\|_0 &\le Ch(\nu + \alpha)\|\nabla e\|_0 + Ch\|p - p_h\|_0 + C\alpha h^2|u|_3 + C(\|\nabla e\|_0 + h)\|\nabla e\|_0 \\ &\le Ch(1+\alpha)\|\nabla e\|_0 + C\|\nabla e\|_0^2 + C\alpha h^2 + Ch\|p - p_h\|_0. \quad \square \end{aligned} \tag{62}$$

Corollary 4.3. *The statement of Theorem 4.3, the results of Corollaries 4.1 and 4.2 imply that*

$$\|u - u_h\|_0 \le C(h^3 + \alpha^{\frac{1}{2}} h^2). \tag{63}$$

In particular,

$$\|u - u_h\|_0 \le Ch^3, \quad \text{if } \alpha = h^2, \tag{64}$$

where C is independent of α and h.

Theorem 4.4. *If the subgrid term Eq. (23) is adopted, we have the following error estimates*

$$\|u - u_h\|_0 + h(\|\nabla(u - u_h)\|_0 + \|p - p_h\|_0) \le C_l h^3, \tag{65}$$

where $\alpha_l = h^2$ in Eq. (23) and C_l is independent of α_l and h.

Proof. The proof is analogous to proofs about the subgrid term Eq. (21). □

5. Numerical tests

In this section, we assess the given two kinds of SGS model by several tests and validate the error analysis results. Meanwhile, we apply the given SGM model to the nonstationary NSEs and implement the simulations of the High Reynolds number flows.

Firstly, we give the algorithm used to deal with the nonlinear term and the SGS eddy viscosity term for the stationary NSEs. For the nonlinear term, the Newtonian iterative method is adopted [9]. Given $(u_h^{n-1}, p_h^{n-1}) \in (X_h, Q_h)$, we find $(u_h^n, p_h^n) \in (X_h, Q_h)$ $(\forall\ (v_h, q_h) \in (X_h, Q_h))$ satisfying

$$\begin{aligned} &\nu a(u_h^n, v_h) - d(v_h, p_h^n) + d(u_h^n, q_h) + M(u_h^n, v_h) + b(u_h^n; u_h^{n-1}, v_h) + b(u_h^{n-1}; u_h^n, v_h) \\ &\quad = (f, v_h) + b(u_h^{n-1}; u_h^{n-1}, v_h). \end{aligned} \tag{66}$$

In order to calculate the SGS term (21) based on the elliptic projection, we can rewrite the SGS term as follows

$$\begin{aligned} M(u_h^n, v_h) &= \alpha(\nabla(I - P_{1,h})u_h^n, \nabla(I - P_{1,h})v_h) \\ &= \alpha(\nabla(I - P_{1,h})u_h^n, \nabla v_h) - \alpha(\nabla(I - P_{1,h})u_h^n, \nabla P_{1,h} v_h) \\ &= \alpha(\nabla u_h^n, \nabla v_h) - \alpha(\nabla P_{1,h} u_h^n, \nabla v_h). \end{aligned} \tag{67}$$

In the framework of the Newtonian iteration, this elliptic SGS term is described by

$$M(u_h^n, v_h) = \alpha(\nabla u_h^n, \nabla v_h) - \alpha(\nabla P_{1,h} u_h^{n-1}, \nabla v_h). \tag{68}$$

The term $P_{1,h}u_h^{n-1}$ is obtained by the solution of the Laplace equation approximated by piecewise linear functions, although a transformation relation between L^2 projection and elliptical projection is offered.

If the subgrid term $M(u_h^n, v_h)$ in Eq. (66) is substituted by $M_l(u_h^n, v_h)$, the subgrid term can be rewritten by

$$M_l(u_h^n, v_h) = \alpha(\nabla(u_h^n - Q_{1,h}u_h^n), \nabla(v - Q_{1,h}v_h)). \tag{69}$$

In the framework of Newtonian iteration, the L^2 SGS term is calculated by

$$M_l(u_h^n, v) = \alpha(\nabla(u_h^n - Q_{1,h}u_h^{n-1}), \nabla(v - Q_{1,h}v_h)). \tag{70}$$

Since $Q_{1,h}$ is the L^2 projection, $Q_{1,h}u_h^{n-1}$ and $Q_{1,h}v_h$ can be denoted directly in the R_1 finite element space [14].

5.1. Example of a exact solution

It is essential to investigate the SGS model (21) and (23) for low viscosity fluid flow and validate the flexibility and convergence rates of this model. So, we need to choose a true solution. We consider Eq. (1) on the domain $\Omega = [0, 1] \times [0, 1]$, with a body force obtained such that the following true solution is given by $u = (u_1, u_2)$,

$$\begin{cases} u_1 = 2x^2(x-1)^2 y(y-1)(2y-1), \\ u_2 = -2y^2(y-1)^2 x(x-1)(2x-1), \\ p = y^2 - x^2. \end{cases} \tag{71}$$

The viscosity $\nu = 0.01$. The mesh scales $h \in \{1/20, 1/30, 1/40, 1/50\}$. The iterative tolerance is 10^{-8}. In Figs. 1 and 2, we show the convergence orders by log–log plots. It is shown that the convergence orders of the elliptic projection SGS

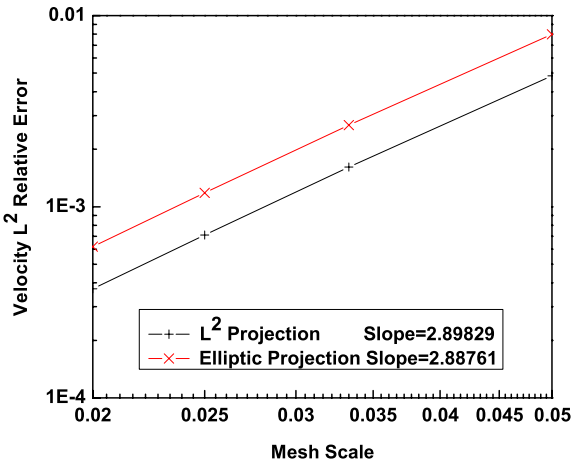

Fig. 1. L^2 convergence order of velocity field by a log–log plot.

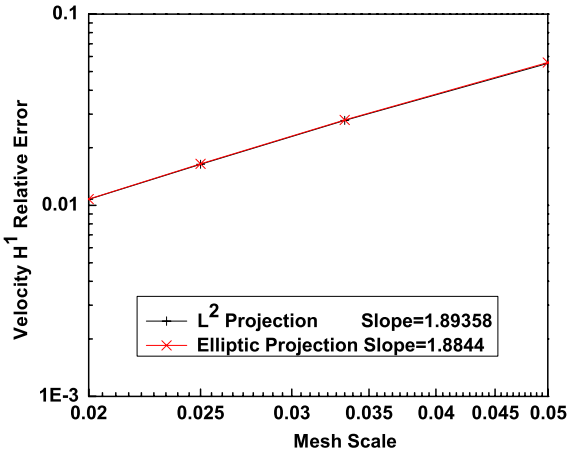

Fig. 2. H^1 convergence order of velocity field by a log–log plot.

method are up to 2.88761 and 1.8844 for L^2 and H^1 norms of velocity fields, respectively. The convergence orders of the L^2 projection SGS method are up to 2.89829 and 1.89358 for L^2 and H^1 norms of velocity fields, respectively. From Figs. 1 and 2, it is exhibited that the numerical results agree with the exact solution very well. According to these results, we know that the SGS terms for low Reynolds number fluid flows do not act on the large scale structures. Meanwhile, the obtained results support the theoretical analysis. On the other hand, the computational results by L^2 SGS model are better than those by elliptic SGS model.

5.2. Lid-driven cavity fluid flows

The drawbacks of usual Galerkin methods for convection dominated problems are well known and well documented [6]. In this part, the proposed models are applied to simulate the benchmark lid-driven cavity fluid flows of high Reynolds fluid flows and try out the correctness of the models. The investigations are to show that the SGS models give high quality, coarse mesh solutions compared with the benchmark, fine mesh results of Ghia [15]. The computational domain $\Omega = [0, 1]\times[0, 1]$ and the top boundary velocity $(u, v) = (1, 0)$, and the other three boundaries are non-slip boundary conditions. The iterative tolerance is 10^{-6}. The Reynolds numbers $Re = LU/\nu = 1000$ and the mesh scale $h = 1/40$. It is known that if we do not adopt the subgrid models, it is impossible to implement simulation successfully on this kind of coarse mesh [6]. The comparisons of the numerical solutions (the SGS numerical solutions and Ghia benchmark solutions [15]) are shown in Fig. 3. From the results, it is clear that the given SGS methods perform very well and are comparable to the results obtained by Ghia on a more refined mesh. Another important result is that the CPU cost of L^2 SGS model accounts for about 70% CPU cost of elliptic SGS model. From this point of view, the L^2 SGS model is superior to the elliptic SGS model.

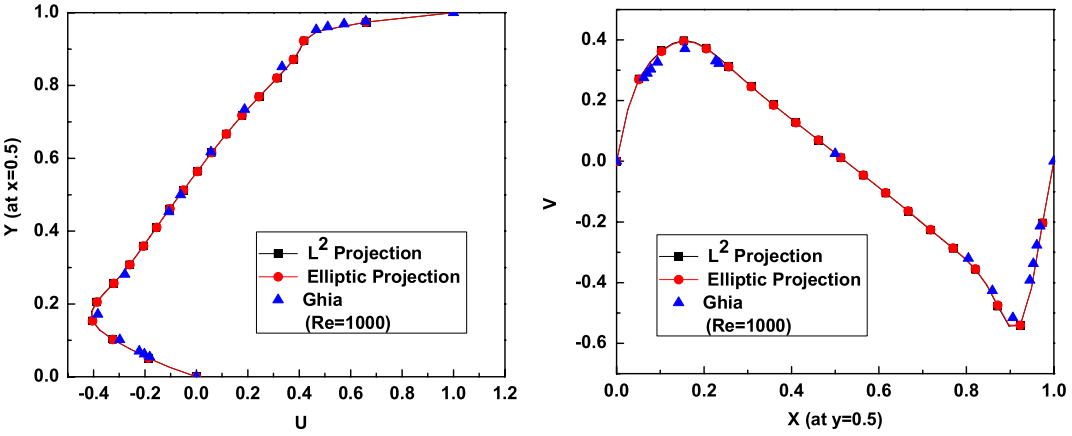

(a) Horizontal velocity profiles. (b) Vertical velocity profiles.

Fig. 3. The numerical solutions and the benchmark solution.

5.3. *Fluid flows around a cylinder by high Reynolds numbers*

In this part, we investigate the two-dimensional under-resolved fluid flow around a cylinder by the proposed SGS models. In this kind of fluid flows, the flow patterns are affected by the interaction of the fluid flows with two parallel planes and the surface of the cylinder. This problem is very useful to validate the SGS models by vortex street patterns. The success and failure of the SGS models simulations are useful for real fluid flows and engineering applications.

The height of the channel $H = 1$ and the width W are equal to 6 or 8 for $Re = 10^3$ and $Re = 10^6$, respectively. The origin of the cylinder is at $(x, y) = (1, 0.5)$ and the radius R is equal to 0.15. The time-dependent inlet flow velocity profiles are given by

$$\begin{cases} u_1(0, y, t) = -6y(y - H)/H^3, \\ u_2(0, y, t) = 0, \end{cases}$$

and the boundary condition of the outlet is set as

$$\frac{\partial u}{\partial n} = 0.$$

The boundary conditions of the two parallel planes and the cylinder surface are set as the non-slip boundary conditions. If the diameter D of the cylinder is chosen as the characteristic length and the mean velocity U_{mean} of inlet as the characteristic velocity, the Reynolds number is defined by $Re = U_{mean}D/\nu$.

The comparisons among three kinds of SGS models (Current model, Guermond–Marra–Quartapelle (GMQ) model [5] and by Kaya–Layton–Riviere (KLR) model [6,7]) are investigated for fluid flows around a cylinder. These investigations will address the actions of SGS models on large scale flow structures. Now, we introduce the GMQ model and KLR model. The GMQ model is based on the two-level Lagrange finite element setting, which is defined by [5]

$$S_{GMQ}(u_h^H, v_h^H) = c_b \sum_{K \in \tau_k} \sqrt{|K|} \int_K \nabla u_h^H \cdot \nabla v_h^H,$$

where $|K|$ is the measure of K, $u_h^H = (1 - P_H)u_h$ and $v_h^H = (1 - P_H)v_h$ (Refer to [5] for the details of the functional settings and the definition of the operator P_H). The KLR model is also based on two-level finite element space, which is defined by [6,7]

$$S_{KLR}(g_H, v_h) = \alpha((\nabla u_h, \nabla v_h) - (g_H, \nabla v_h)),$$

where g_H is the L^2 projection of ∇u^h

$$(g_H - \nabla u_h, l_H) = 0.$$

α is a user-selected stabilization parameter and typically, $\alpha = \mathcal{O}(h)$ (Refer to [6,7] for the details of the functional settings). In the numerical computations, the iterative scheme is adopted to implement these two subgrid models [6].

In order to implement the Galerkin method (finite element direct numerical simulation (FEDNS)) under the current computer capability and limited hardware resources, the Reynolds number is set to equal 10^3. By this Reynolds number, we give the comparison results among referred four different methods. The time interval $\Delta t = 0.001$. The mesh scale $h = 1/50$ for Galerkin method and $h = 1/16$ for these two kinds of SGS models. The mesh scale of Galerkin method is enough to resolve the small scale of current flow structures ($h \propto Re^{-1/2}$) [2]. From Figs. 4 and 5, it is very clear that the

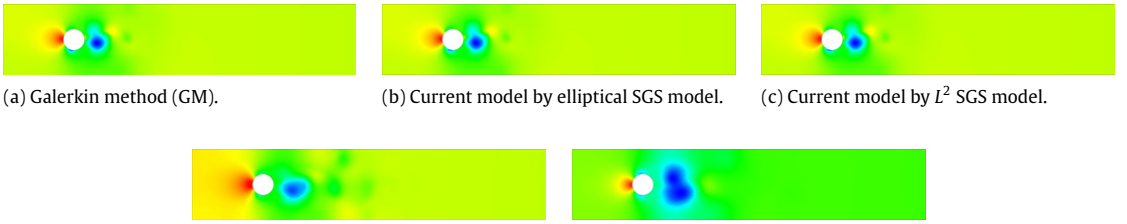

(a) Galerkin method (GM). (b) Current model by elliptical SGS model. (c) Current model by L^2 SGS model.

(d) GMQ model. (e) KLR model.

Fig. 4. The contour patterns of pressure fields ($t = 1$): (a) Galerkin method (GM); (b) Current model by elliptical projection; (c) Current model by L^2 projection; (d) GMQ model; (e) KLR model.

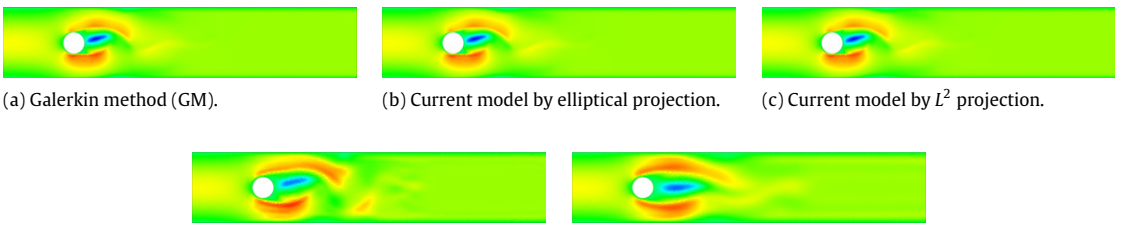

(a) Galerkin method (GM). (b) Current model by elliptical projection. (c) Current model by L^2 projection.

(d) GMQ model. (e) KLR model.

Fig. 5. The contour patterns of horizontal velocity fields ($t = 1$): (a) Galerkin method (GM); (b) Current model by elliptical projection; (c) Current model by L^2 projection; (d) GMQ model; (e) KLR model.

(a) $t = 8$. (b) $t = 9$.

Fig. 6. The vortex shedding patterns by L^2 SGS model: (a) $t = 8$; (b) $t = 9$;.

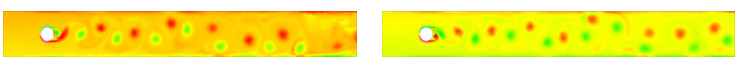

(a) $t = 8$. (b) $t = 9$.

Fig. 7. The vortex shedding patterns by elliptic SGS model: (a) $t = 8$; (b) $t = 9$;.

proposed subgrid models in this paper predicts the flow structures best, compared with the other two subgrid models based on the Galerkin benchmark solutions. From these results, it is proved that the GMQ and KLR subgrid models introduce an overly strong local dissipation into the flow structures, but the current subgrid model presents a suitable local dissipation behavior. The analogous results are addressed by the investigations in our recent paper [16].

In order to assess performance of the current SGS models, the very high Reynolds number ($Re = 10^6$) are chosen to implement the computations of complex flow phenomena. In Figs. 6 and 7, the snapshots of vortex shedding are given. It is obvious that under these very high Reynolds numbers, the flow structures are complex and develop into the two-dimensional turbulence. The vortex filaments are clearly visible. These results demonstrate that the proposed SGS models are effective and flexible.

6. Conclusion

In this paper, we investigate two kinds of subgrid models to simulate high order Reynolds number fluid flows by a $P2/P1$ finite element pair. The theoretical analysis of this method is based on some regular assumptions. The analysis guarantees that the proposed SGS terms do not act on the large scale structures of fluid flows. In fact, these methods can be regarded as a kind of large eddy simulation method. The stability and the error estimates are established.The proposed SGS models are simple and easily implemented. According to computational results, the SGS models provide some creditability to engineering applications. The current numerical tests are based on P_2/P_1 polynomial interpolations. From a computational view, it is clear that the L^2 SGS model is superior to the elliptic SGS model for numerical aspects. In future, these SGS models will attempt to implement some simulations and research for transient 3D high Reynolds fluid flows.

References

[1] V. John, Large Eddy Simulation of Turbulent Incompressible Flows, Springer-Verlag, Berlin, Heidelberg, 2004.
[2] U. Frisch, S.A. Orszag, Turbulence: Challenges for theory and experiment, Phys. Today (1990) 24–32.
[3] T. Iliescu, W.J. Layton, Approximating the larger eddies in fluid motion. III. The Boussinesq model for turbulent fluctuations, An. Ştiinţ. Univ. Al. I. Cuza Iaşi., Mat. (N.S.) 44 (1998) 245–261.
[4] J. Smagorinsky, General circulation experiments with the primitive equation, I: The basic experiment, Mon. Weather Rev. 91 (1963) 99–164.
[5] J.-L. Guermond, A. Marra, L. Quartapelle, Subgrid stabilized projection method for 2D unsteady flows at high Reynolds numbers, Comput. Methods Appl. Mech. Engrg. 195 (2006) 5857–5876.
[6] S. Kaya, W. Layton, B. Rivière, Subgrid stabilized defect correction methods for the Navier–Stokes equations, SIAM J. Numer. Aanal. 44 (4) (2006) 1639–1654.
[7] V. John, S. Kaya, Finite element error analysis of a variational multiscale method for the Navier–Stokes equations, Adv. Comput. Math. 28 (2008) 43–61.
[8] T.J.R. Hughes, L. Mazzei, K.E. Jansen, Large eddy simulation and the variational multiscale method, Comput. Visual. Sci. 3 (2000) 47–59.
[9] Yinnian He, Aiwen Wang, A simplified two-level method for the steady Navier–Stokes equations, Comput. Methods Appl. Mech. Engrg. 197 (2008) 1568–1576.
[10] R. Temam, Navier–Stokes Equations, Theory and Numerical Analysis, NorthHolland, Amsterdam, 1983.
[11] V. Girault, P.A. Raviat, Finite Element Methods for Navier–Stokes, in: Springer Series in Computational Mathematics, vol. 5, Springer-Verlag, Berlin, 1986.
[12] A. Quarteroni, A. Valli, Numerical Approximation of Partial Differential Equations, Springer-Verlag, World Publishing Co., 1998.
[13] W. Layton, A connection between subgrid-scale eddy viscosity and mixed methods, Appl. Math. Comput. 133 (1) (2002) 147–157.
[14] S. Kaya, B. Riviére, A two-grid stabilization method for solving the steady-state Navier–Stokes equations, Inc. Numer. Methods Partial Differential Equations 22 (2005) 728–743.
[15] U. Ghia, K.N. Ghia, C.T. Shin, High–Re solutions for incompressible flow using the Navier–Stokes equations and a multigrid method, J. Comput. Phys. 48 (1982) 387–411.
[16] Yinnian He, Yan Zhang, A subgrid model for the time-dependent Navier–Stokes equations, Adv. Numer. Anal. (2009) doi:10.1155/2009/494829.